European Review for Medical and Pharmacological Sciences 2021; 25: 2235-2244

MicroRNA related prognosis biomarkers from high throughput sequencing data of kidney renal papillary cell carcinoma

Z.-Y. YAO[1], C.-Q. XING[2], T. ZHANG[1], Y.-W. LIU[3], X.-L. XING[1]

[1]Hunan Provincial Key Laboratory for Synthetic Biology of Traditional Chinese Medicine, Hunan University of Medicine, Huaihua, Hunan, P. R. China
[2]The First Affiliated Hospital of Hunan University of Medicine, Huaihua, Hunan, P. R. China
[3]Beijing Advanced Innovation Center for Food Nutrition and Human Health, China Agricultural University, Beijing, China

Zhi-Yong Yao and Chaoqun Xing contributed equally to this work

Abstract. – OBJECTIVE: Renal cell carcinoma (RCC) is the most common type of kidney cancer which could be mainly classified as kidney renal clear cell carcinoma (KIRC) and kidney renal papillary cell carcinoma (KIRP). KIRP ranks second in terms of morbidity rate which comprised 10%-15% of patients. Till now, there were few biomarkers could forecast the outcomes of KIRP. The aim of this study was to identify novel prognostic biomarkers to predict clinical outcomes for KIRP.

MATERIALS AND METHODS: In this study, we firstly downloaded 326 miRNAs (35 controls vs. 291 patients), 321 mRNAs (33 controls vs. 288 patients) data and their corresponding clinical information from The Cancer Genome Atlas database. Then, we used DESeq2 analysis, univariate and multivariate Cox regression analysis, pathologic MNT correlation analysis, and specific prognostic model analysis to identify the potential prognosis biomarkers.

RESULTS: We found 25 differential expression miRNAs (DEMs) and 7 differential expression genes (DEGs) were associated with the overall survival rates of KIRP patients. After multivariate Cox regression analysis, we established 2 prognostic prediction models and calculated the area under the 1-, 3-, and 5-year curve (AUC) values of DEMs and DEGs respectively. Among them, the prognostic index (PI) of DEMs and DEGs showed good predictive ability which was 0.8293/0.7205, 0.8148/0.7301 and 0.7776/0.6810 respectively.

CONCLUSIONS: In this study, we found that 3 DEMs and 2 DEGs could be used as prognostic biomarkers to predict the outcome for KIRP. Our study was just a primary analysis based on high-throughput sequencing and clinical information.

Key Words:
KIRP, MiRNAs, mRNAs, Prognostic biomarker.

Introduction

Renal cell carcinoma (RCC) is the most common type of kidney cancer which ranks sixth in males and eighth in females among all types of tumors[1]. Kidney is a complex organ which made up of various types of cells. Therefore, RCC can be classified to kidney renal clear cell carcinoma (KIRC), kidney renal papillary cell carcinoma (KIRP) and chromophobe renal cell carcinoma (KICH) according to the cell types in kidney[2]. Among these different subtypes, KIRC has the highest mortality rate, followed by KIRP which comprised of 10%-15% of cases[2]. 70% of RCC is localized or locally advanced at diagnosis[2]. Surgery is a very effective manner for localized RCC. However, recurrence is very common after surgery because of metastasis. More recently, researchers[3,4] show that 30-35% of localized RCC will finally develop to distant metastases which indicate that the prognosis of RCC remains poor.

Currently, several biomarkers for KIRC are able to forecast the medical effectiveness and outcomes, such as von Hippel-Lindau, vascular endothelial growth factor, carbonic anhydrase IX, and hypoxia-inducible factor 1 alpha/2 alpha[5-10]. However, there are few biomarkers could be used efficiently in the prognosis of KIRP. Finding suitable prognostic biomarkers for KIRP is very urgently in clinical diagnosis.

Corresponding Authors: Yuan-Wu Liu, Ph.D; e-mail: yuanwu_liu@126.com
Xiao-Liang Xing, Ph.D; e-mail: xiaoliangxinghnm@126.com

MicroRNAs (miRNAs) are short non-coding RNAs with 19-24 nt in length. MiRNAs is highly conserved in species and regulates the expression of target mRNAs by partially or fully complementary binding degradation. Increasing evidence suggest that miRNAs are involve in series of fundamental cellular processes, including cell differentiation, proliferation, and apoptosis, as well as carcinogenesis or cancer progression[11]. Aberrant expression of miRNA plays an important role in the pathogenesis of various diseases, including cancers[12-15]. A large number of miRNAs and miRNA related mRNAs have also been identified as prognostic biomarkers for various cancers.

The Cancer Genome Atlas (TCGA) is an open access database collects more than 20,000 samples covering 33 different cancer types. Most samples in TCGA database contain mRNAs expression data, miRNAs expression data and standardized clinical data. In the present study, we aim to identify prognostic biomarkers for KIRP, which associated with aberrant expression of miRNAs, through related TCGA data analysis.

Materials and Methods

Differentially Expression Screening

All of these data used in the present study were obtained from a public database, The Cancer Genome Atlas database (TCGA) (https://portal.gdc.cancer.gov/). We used DESeq2 package in R software to analyze the mRNAs/miRNAs expression profiles by setting the threshold as p-adj < 0.01, |logFC| ≥ 1 and basemean > 50. The normalized expression data of miRNA and mRNA were output for further survival and correlation analysis. All figures were performed by Graphpad Prism 6.01 (San Diego, CA, USA).

Correlation and Functional Enrichment Analysis

In this study, overlap genes between the target genes of DEMs and DEGs were used for the spearman correlation analysis. The threshold for correlation analysis was set as p-value < 0.05 and r < -0.3. We performed GO and KEGG analysis by DAVID 6.8[16]. All figures were performed by GraphPad Prism 6.01 (San Diego, CA, USA) and Cytoscape_3.7.2 software (Toronto, Canada).

Survival Analysis

KIRP patients were transformed into low expression group and high expression group dependent on the median value. We used RegParallel and survival packages in R to carry out univariate Cox regression analysis. We used IBM SPSS 22 (Armonk, New York, USA) software to carry out multivariate Cox regression analysis. The target miRNAs/mRNAs were considered to be significantly correlated with the survival curve when the p-value of miRNAs/mRNAs was less than 0.05. All figures were performed by GraphPad Prism 6.01 (San Diego, CA, USA).

Pathologic MNT Correlation Analysis

Pathologic M was divided into M0 group and M1 group dependent on the distant metastasis status. Pathologic N was divided into N0 group and N1+2 group dependent on the lymph node metastasis status. Pathologic T was divided into T1+2 group and T3+4 group dependent on the tumor size and infiltrating range status. And then, we used Kaplan-Meier analysis to exam the correlation of overall survival (OS) with pathologic MNT, and then used unpaired two-tail Student's t-test to exam the correlation of target DEGs with pathologic MNT. All figures were performed by GraphPad Prism 6.01 (San Diego, CA, USA).

Construction of the KIRP-Specific Prognostic Model

Based on the multivariate Cox hazards regression, the DEMs and DEGs signature scores were used to construct the prognostic model, and the prognostic index (PI) of OS was constructed as previous reports[17,18]. KIRP patients were divided into low-risk group and high-risk group with median risk score. And then we constructed time-dependent receiver operating characteristic (ROC) curves within 1-, 3-, and 5- year and estimated the area under the ROC curve (AUC) for DEMs and DEGs. All figures were performed by GraphPad Prism 6.01(San Diego, CA, USA).

Results

Identification of DEMs and DEGs in KIRP

The miRNAs and mRNAs expression data and the clinical information data of KIRP were obtained from open access database TCGA. There were 326 (35 controls *vs.* 291 patients) miRNA expression data and 321 (33 controls *vs.* 288 patients) mRNA expression data. By using DESeq2 with the cut-off criteria of p-adj < 0.01, |logFC| ≥ 1 and basemean > 50, we identified 77 DEMs (32 upregulated DEMs and 45 downregulated

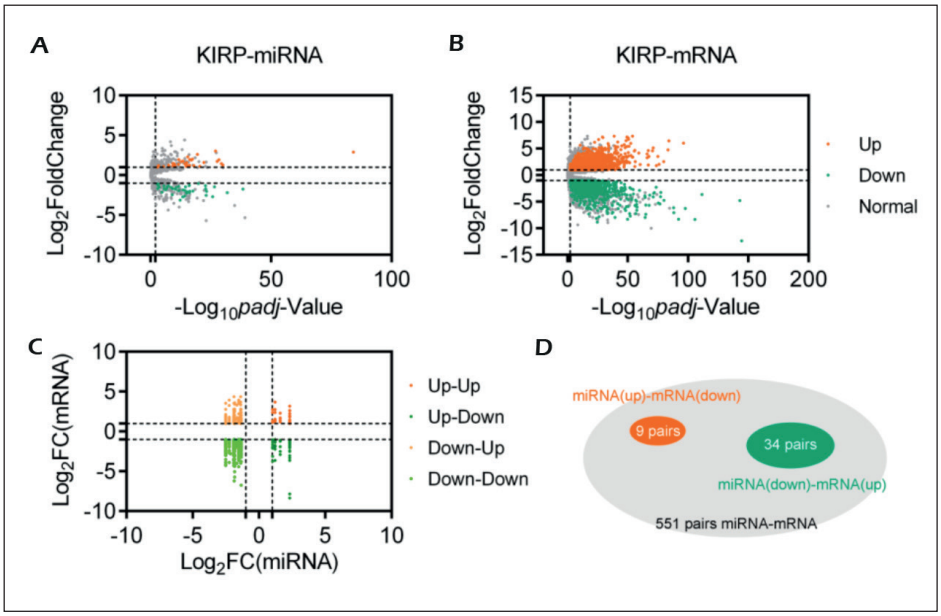

Figure 1. Differentially expressed miRNAs and mRNA for KIRP. **A,** Volcano plot of differentially expressed miRNAs for KIRP. **B,** Volcano plot of differentially expressed mRNAs for KIRP. **C,** Scatter plot of Log2FC (miRNA) versus Log2 FC(mRNA) in KIRP. **D,** Verified negative correlation of 43 pair miRNA-mRNA.

DEMs) (Figure 1A, **Supplementary Table I**) and 4013 DEGs (2327 up-regulated DEGs and 1686 down-regulated DEGs) (Figure 1B, **Supplementary Table II**).

For those 77 DEMs we carried out univariate Cox regression analysis and identified 25 DEMs were significantly correlated with OS of KIRP (Table I). Of which 6 DEMs (hsa-miR-34a-5p, hsa-miR-181c-5p, hsa-miR-486-5p, hsa-miR-584-5p, hsa-miR-144-5p, and hsa-miR-1180-3p) were up-regulated and 19 DEMs (hsa-miR-10b-3p, hsa-miR-126-3p, hsa-miR-127-3p, hsa-miR-127-5p,

Table I. Prognostic DEMs for KIRP by univariate Cox regression analysis.

miRNA	*p*	LogRank	HR	HRlower	HRupper
hsa-miR-10b-3p	0.031	0.027	2.05	1.07	3.94
hsa-miR-1180-3p	0.024	0.021	0.49	0.27	0.91
hsa-miR-126-3p	0.007	0.006	2.36	1.26	4.41
hsa-miR-127-3p	0.005	0.004	2.52	1.32	4.82
hsa-miR-127-5p	0.006	0.005	2.44	1.29	4.60
hsa-miR-134-5p	0.007	0.005	2.41	1.28	4.55
hsa-miR-141-5p	0.004	0.003	2.52	1.33	4.75
hsa-miR-143-3p	0.017	0.014	2.14	1.15	4.00
hsa-miR-143-5p	0.022	0.019	2.08	1.11	3.89
hsa-miR-144-5p	0.013	0.011	0.46	0.25	0.85
hsa-miR-145-3p	0.008	0.007	2.39	1.25	4.57
hsa-miR-145-5p	0.002	0.001	2.84	1.46	5.52
hsa-miR-181c-5p	0.015	0.013	0.47	0.25	0.86
hsa-miR-199a-3p	0.005	0.004	2.53	1.32	4.84
hsa-miR-199a-5p	0.009	0.007	2.33	1.24	4.41
hsa-miR-199b-3p	0.005	0.004	2.53	1.32	4.84
hsa-miR-199b-5p	0.008	0.006	2.38	1.26	4.49
hsa-miR-217-5p	0.003	0.002	2.71	1.40	5.27
hsa-miR-24-1-5p	0.015	0.013	0.45	0.23	0.86
hsa-miR-3065-3p	0.029	0.026	1.99	1.07	3.67
hsa-miR-34a-5p	0.000	0.000	0.27	0.13	0.54
hsa-miR-379-5p	0.001	0.000	3.25	1.64	6.44
hsa-miR-381-3p	0.001	0.001	2.95	1.52	5.74
hsa-miR-486-5p	0.014	0.012	0.46	0.25	0.85
hsa-miR-584-5p	0.014	0.012	2.19	1.17	4.09

Table II. The spearman correlation analysis for miRNAs-mRNAs.

miRNA	Gene	p	R	miRNA	Gene	p	R
hsa-miR-10b-3p	BRSK1	0.00	-0.40	hsa-miR-145-5p	FMNL2	0.00	-0.33
hsa-miR-10b-3p	HLA-B	0.00	-0.31	hsa-miR-145-5p	ITGB8	0.00	-0.49
hsa-miR-10b-3p	HLA-G	0.00	-0.36	hsa-miR-145-5p	ONECUT2	0.00	-0.34
hsa-miR-10b-3p	PRAME	0.00	-0.41	hsa-miR-145-5p	SEL1L3	0.00	-0.33
hsa-miR-10b-3p	RAP2B	0.00	-0.33	hsa-miR-145-5p	SEMA6A	0.00	-0.32
hsa-miR-10b-3p	SATB2	0.00	-0.47	hsa-miR-181c-5p	FLT1	0.00	-0.42
hsa-miR-1180-3p	NRN1	0.00	-0.61	hsa-miR-181c-5p	KAT2B	0.00	-0.33
hsa-miR-127-5p	ITGB8	0.00	-0.31	hsa-miR-181c-5p	PLCL2	0.00	-0.32
hsa-miR-127-5p	RPGRIP1L	0.00	-0.34	hsa-miR-199a-3p	ITGB8	0.00	-0.40
hsa-miR-134-5p	NSUN5	0.00	-0.33	hsa-miR-199a-3p	NUTF2	0.00	-0.31
hsa-miR-134-5p	RIMS2	0.00	-0.30	hsa-miR-199a-3p	PHYHIPL	0.00	-0.37
hsa-miR-143-3p	ITGB8	0.00	-0.44	hsa-miR-199a-3p	SERPINE2	0.00	-0.46
hsa-miR-143-3p	TAPBP	0.00	-0.34	hsa-miR-199a-3p	TNIK	0.00	-0.38
hsa-miR-145-3p	ARMC3	0.00	-0.40	hsa-miR-34a-5p	NOS1AP	0.00	-0.36
hsa-miR-145-3p	CCDC40	0.00	-0.41	hsa-miR-34a-5p	SYT9	0.00	-0.32
hsa-miR-145-3p	CREB5	0.00	-0.55	hsa-miR-34a-5p	WSCD2	0.00	-0.37
hsa-miR-145-3p	DGKH	0.00	-0.38	hsa-miR-381-3p	DGKH	0.00	-0.31
hsa-miR-145-3p	KLF8	0.00	-0.44	hsa-miR-381-3p	DMTF1	0.00	-0.30
hsa-miR-145-3p	PTGFRN	0.00	-0.35	hsa-miR-381-3p	WNT5A	0.00	-0.33
hsa-miR-145-3p	ZNF385B	0.00	-0.40	hsa-miR-584-5p	CALB1	0.00	-0.34
hsa-miR-145-5p	ARL6IP5	0.00	-0.41	hsa-miR-584-5p	FREM1	0.00	-0.30
hsa-miR-145-5p	CREB5	0.00	-0.58				

hsa-miR-134-5p, hsa-miR-141-5p, hsa-miR-143-3p, hsa-miR-143-5p, hsa-miR-145-3p, hsa-miR-145-5p, hsa-miR-199a-3p, hsa-miR-199a-5p, hsa-miR-199b-3p, hsa-miR-199b-5p, hsa-miR-217-5p, hsa-miR-24-1-5p, hsa-miR-3065-3p, hsa-miR-379-5p, and hsa-miR-381-3p) were downregulated. Followed by DEMs survival analysis, we used miRDB and TargetScanHuman 7.2 to predict the putative target genes of those 25 DEMs. By Venn analysis for those 25 DEMs target genes cross to the DEGs in KIRP, we identified 551 pairs miRNAs-mRNAs correlated with 16 DEMs and 457 DEGs (Figure 1C).

The mainly expression and regulation pattern between miRNAs and mRNAs is negative correlation. Thus, to further narrow-down the target genes, we introduced spearman correlation analysis and found there were 43 pairs miRNAs-mRNAs involved 38 overlap DEGs which were negatively correlated with 12 DEMs (Figure 1D, Table II).

Functional Enrichment Analyses

The spearman correlation analysis showed there were 38 overlap DEGs which correlated with 12 DEMs. Based on this result, we firstly constructed the network relationship between those DEGs and DEMs by Cytoscape_3.7.2 (Figure 2).

To investigate the biological effects, we performed GO and KEGG functional enrichment analysis. There were 6 cellular components (CC), 13 biological processes (BP), and 2 molecular functions (MF) were enriched (Figure 3A-C). The KEGG functional enrichment analysis showed 9 pathways were enriched, including tumor-related pathways, such as cell adhesion molecules (CAMs) (Figure 3D).

Pathologic MNT Correlation Analysis

Previous reports indicated that pathologic MNT were closely related to OS. We firstly in-

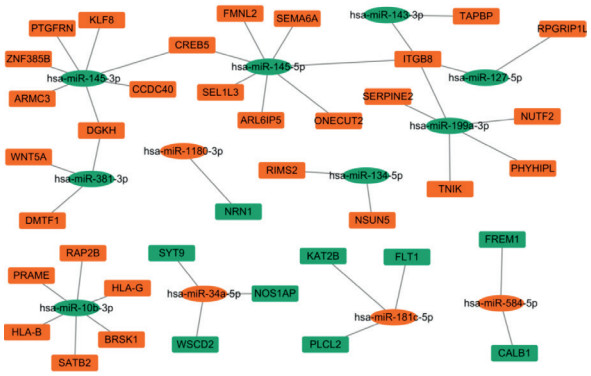

Figure 2. Network of miRNA and related mRNA. Constructed network of miRNA and related mRNA for KIRP. The rectangles and the ellipses represent mRNA and miRNA respectively. Orange and green represent upregulated and downregulated expression respectively.

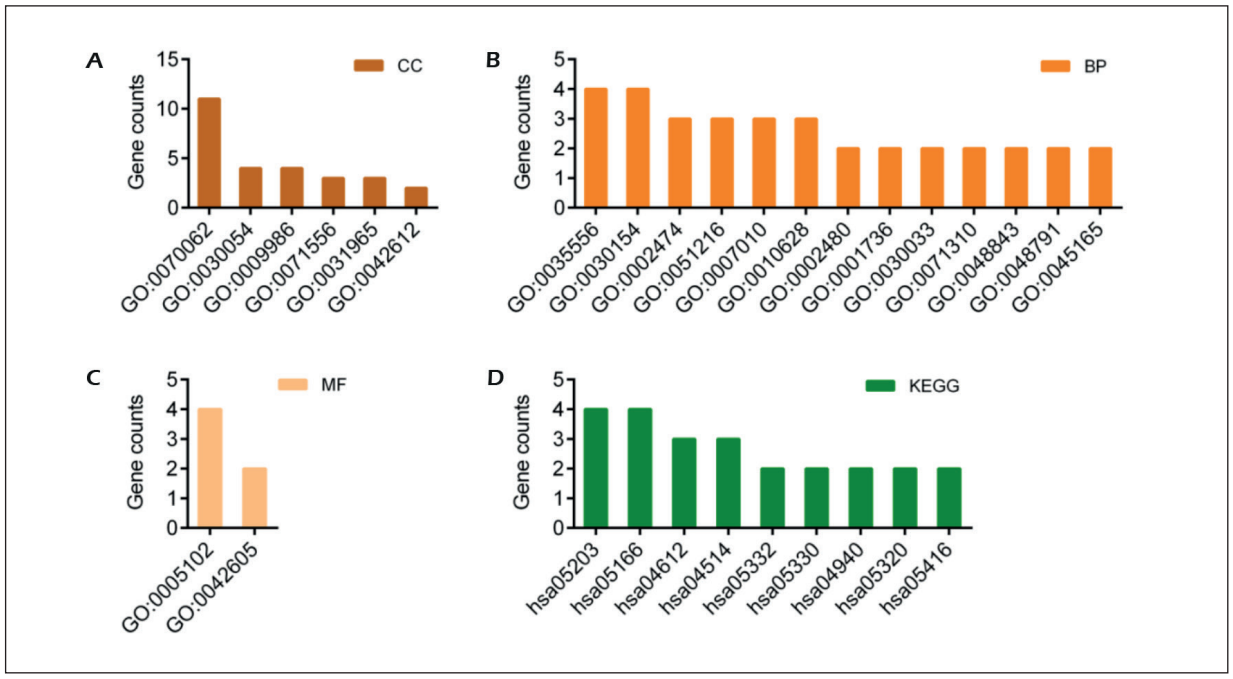

Figure 3. Functional Enrichment Analyses. **A-C,** The enriched CC, BP and MF term analyzed by David 6.8. **D,** The enriched KEGG term analyzed by David 6.8. CC, Cellular Component. BP, Biological Processes. MF, Molecular Functions. KEGG, Kyoto Encyclopedia of Genes and Genomes.

vestigated the correlations of pathologic MNT with OS. These results showed that pathologic MNT were closely associated with the OS for KIRP (Figure 4A-C). Then, we investigated the correlations of 38 overlap DEGs with pathologic MNT. These results indicated that there were 6 overlap DEGs (ZNF385B, ARL6IP5, NUTF2, RIMS2, SATB2, and PRAME) correlated with pathologic M (Figure 4D), 7 overlap DEGs (ITGB8, NOS1AP, ONECUT2, PHYHIPL, RIMS2, SATB2, and ZNF385B) correlated with pathologic N (Figure 4E) and 18 overlap DEGs (ARL6IP5, BRSK1, CALB1, CCDC40, CREB5, DGKH, DMTF1, ITGB8, KLF8, NOS1AP, NRN1, NUTF2, PHYHIPL, RIMS2, SATB2, SEL1L3, WNT5A, and ZNF385B) correlated with pathologic T (Figure 4F). There were only 3 overlap DEGs (RIMS2, SATB2, and ZNF385B) associated with both pathologic MNT.

Establishment of mRNAs/miRNAs Prognostic Models

After pathologic MNT correlation analysis, we evaluated the relationships between those 3 overlap DEGs (RIMS2, SATB2, and ZNF385B) and the OS of KIRP patients. We found SATB2 and ZNF385B were significantly correlated with the OS of KIRP patients (Figure 5A-B). Subsequently, we performed a multivariate regression analysis for those 2 overlap DEGs (SATB2 and ZNF385B) and found those 2 DEGs were still correlated with the OS of KIRP patients. Followed by multivariate regression analysis, we constructed a prognostic model by using those 2 DEGs. As shown in Figure 5C, the patients with low risk actually exhibited a good OS. Subsequently, we predicted 1-, 3-, and 5-year survival rate accurately for KIRP patients. The time-dependent receiver operating characteristic (ROC) curves for those 2 DEGs signature have area under curve (AUC) values higher than 0.5, which were 0.7205, 0.7301, and 0.6810 respectively (Figure 5D-F).

By retrospective examination, we found 3 (hsa-miR-24-1-5p, hsa-miR-34a-5p, and hsa-miR-181c-5p) out of 25 DEMs were correlated with the OS of KIRP patients as measured by the multivariate Cox regression analysis. We also constructed a prognostic model by using those 3 DEMs. As shown in Figure 6A, the patients with low risk actually exhibited a good OS. The time-dependent ROC curves for the 3 DEMs signature have AUC values higher than 0.5, which were 0.8293, 0.8148, and 0.7776 respectively (Figure 6B-D).

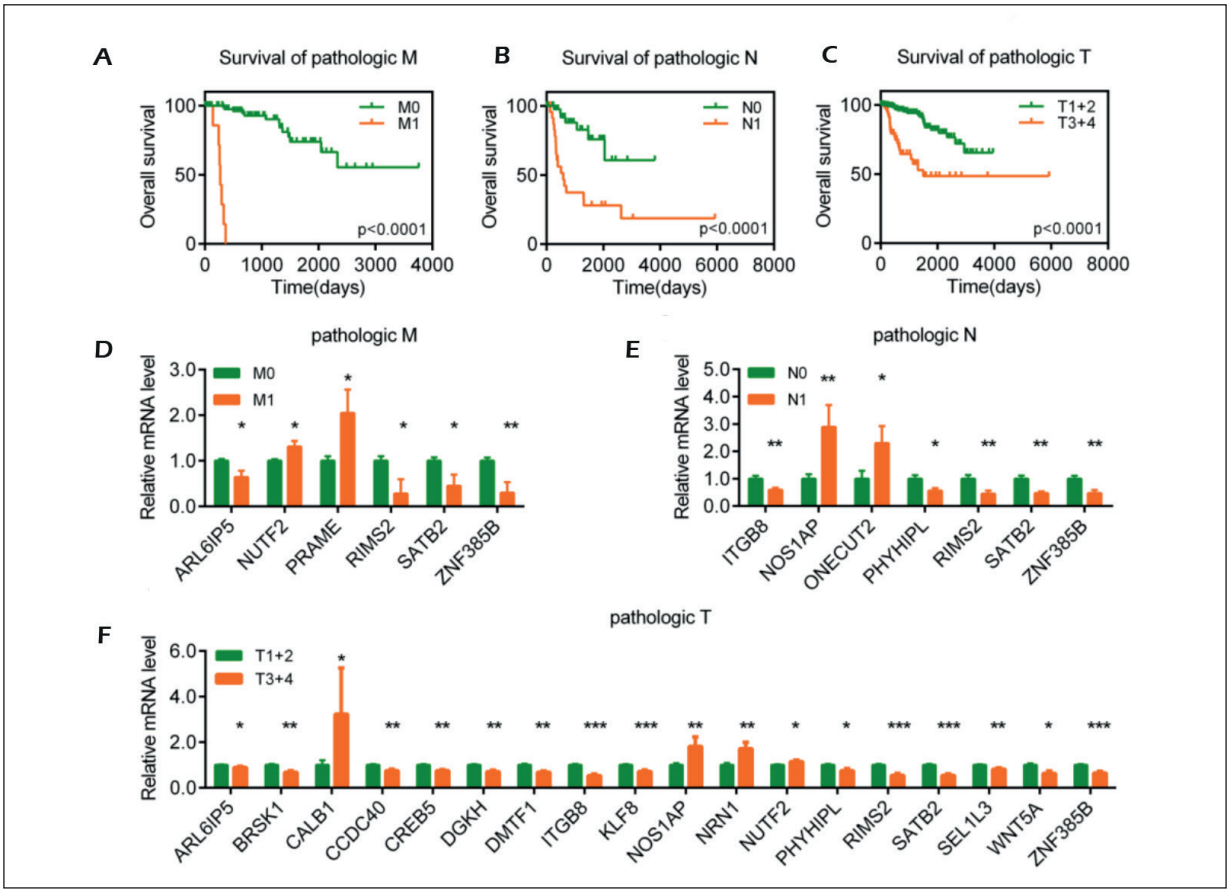

Figure 4. Pathologic MNT correlation analyses. **A-C,** Survival curves of pathologic MNT for KIRP (a,M; b, N; c, T). **D-E,** Associated analyses of overlap DEGs with pathologic M, N, and T stage for KIRP. A repeated-measure ANOVA followed by unpaired two-tail Student's *t* test was used as indicated. All results are expressed as Mean ± SEM.

Discussions

RCC is the most common malignant tumor which ranks the top 10 most prevalence cancer in humans. There are approximately 400,000 new cases and 175,000 deaths around the world in 2018[2]. KIRC is the most prevalence subtype of RCC which followed by KIRP. Several models, such as the University of California, Los Angeles, Integrated Staging System, have been developed to predict the outcomes of KIRC after surgery[19]. The 5-year survival rate of KIRC has shown improvement recently[20]. However, as far as we known, there were few studies to predict the prognosis of KIRP. And more ever, no reliable specific biomarkers have been identified as prognostic biomarkers for KIRP detection and risk stratification.

SATB2 is a transcription factor and chromatin modulator. Previous study indicated that overexpression of SATB2 could lead to tumorigenesis[21]. Another study also indicated SATB2 is highly expressed in pancreatic cancer which could drive pancreatic cancer growth and metastasis[22]. Conner et al (2013)[23] also found skeletal osteosarcomas, osteoblastomas, and osteoid osteomas showed nuclear immunoreactivity for SATB2. Those researches indicated that SATB2 is a hall marker of cancer cells differentiation in benign and malignant tumors which could be used as a diagnostic biomarker. The same with previous researches, our results also supported that SATB2 could be used as diagnostic biomarker in KIRP. Another prognostic biomarker ZNF385B, also called ZNF533, is supposed to be a protein that possesses zinc-finger domains. Elgaaen et al (2012)[24] found that ZNF385B is downregulated and correlated with OS in serous ovarian carcinomas (SOC). But in the present study, we found that ZNF385B was up-regulated and also correlated with OS in KIRP. Differences in the ex-

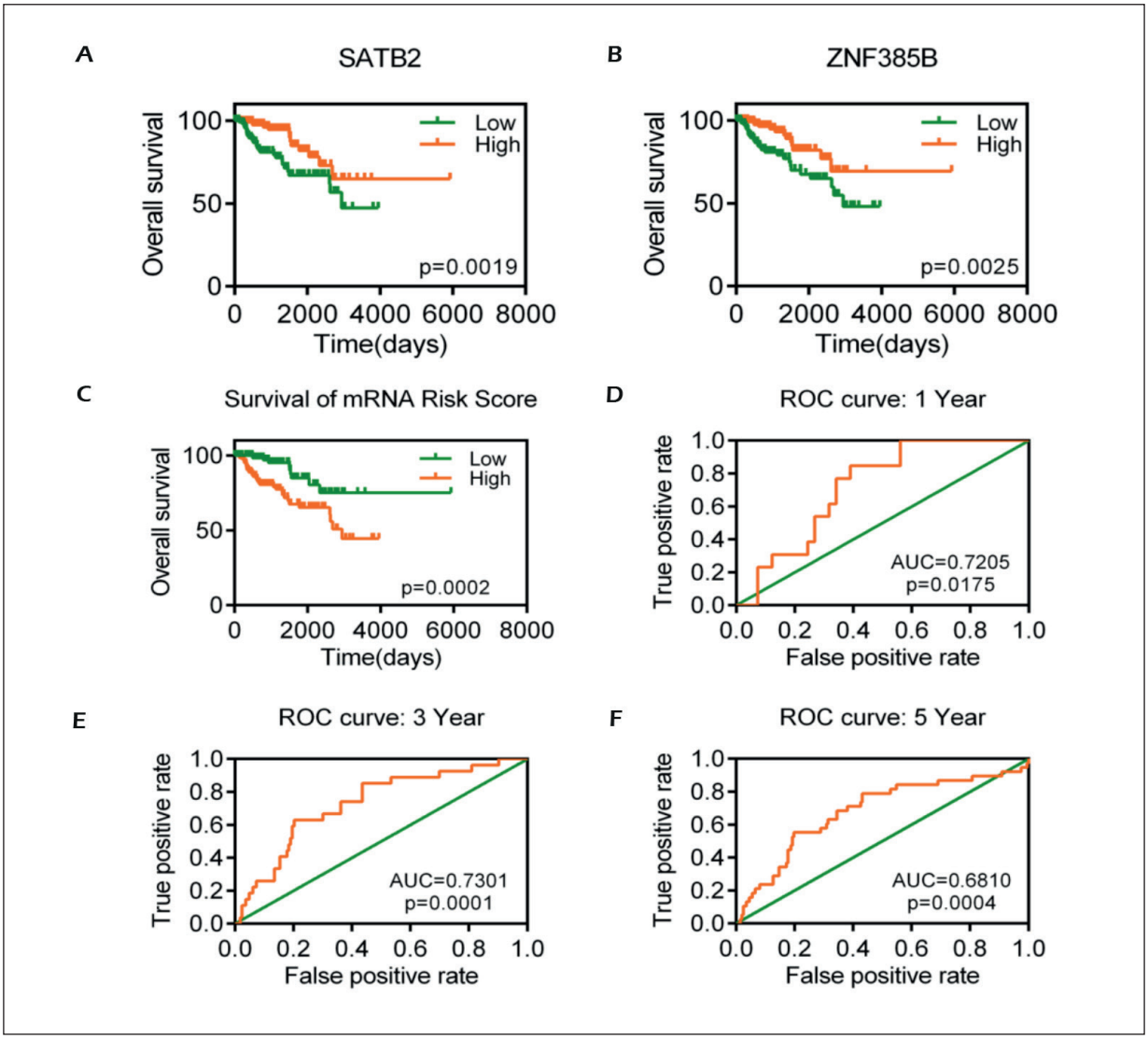

Figure 5. Construction of survival risk score system based on mRNAs signature. **A, B,** Survival curves of target genes (SATB2 and ZNF385B) in KIRP. **C,** The survival curve of patients with high risk and low risk. **D, F,** The ROC curve in 1-year (**D**), 3-year (**E**), and 5-year (**F**) with AUC value.

pression of ZNF385B may be caused by different types of cancer. ZNF385B was associated with OS of SOC and KIRP, suggesting that ZNF385B may play an important role in cancers.

MiRNAs were first identified in 1990s[25]. During the past few decades' research, miRNAs have firmly established the characteristics as key molecular components of normal and pathological cellular states. Due to the stability and universality, miRNAs were considered to be a novel group of disease biomarkers, including cancers[26,27]. In the present study, we comprehensively analyzed the miRNAs expression profile and found 77 DEMs, of which 25 DEMs was correlated with OS of KIRP patients. By cross analysis of DEMs predicted target genes and DEGs followed by spearman correlation analysis, we found 38 DEGs which were associated with 12 DEMs.

Previous studies[28] indicated that cancer stage (MNT) was recognized as one of the strongest prognostic factors in the clinical outcome of patients with cancers. Therefore, we introduced pathologic MNT stage correlation analysis to narrow down the potential prognostic biomarkers. Out of those 38 DEGs, we found that 6 DEGs were correlated with pathologic M, 7 DEGs were correlated with pathologic N, and 18 DEGs were correlated with pathologic T. Based on the mul-

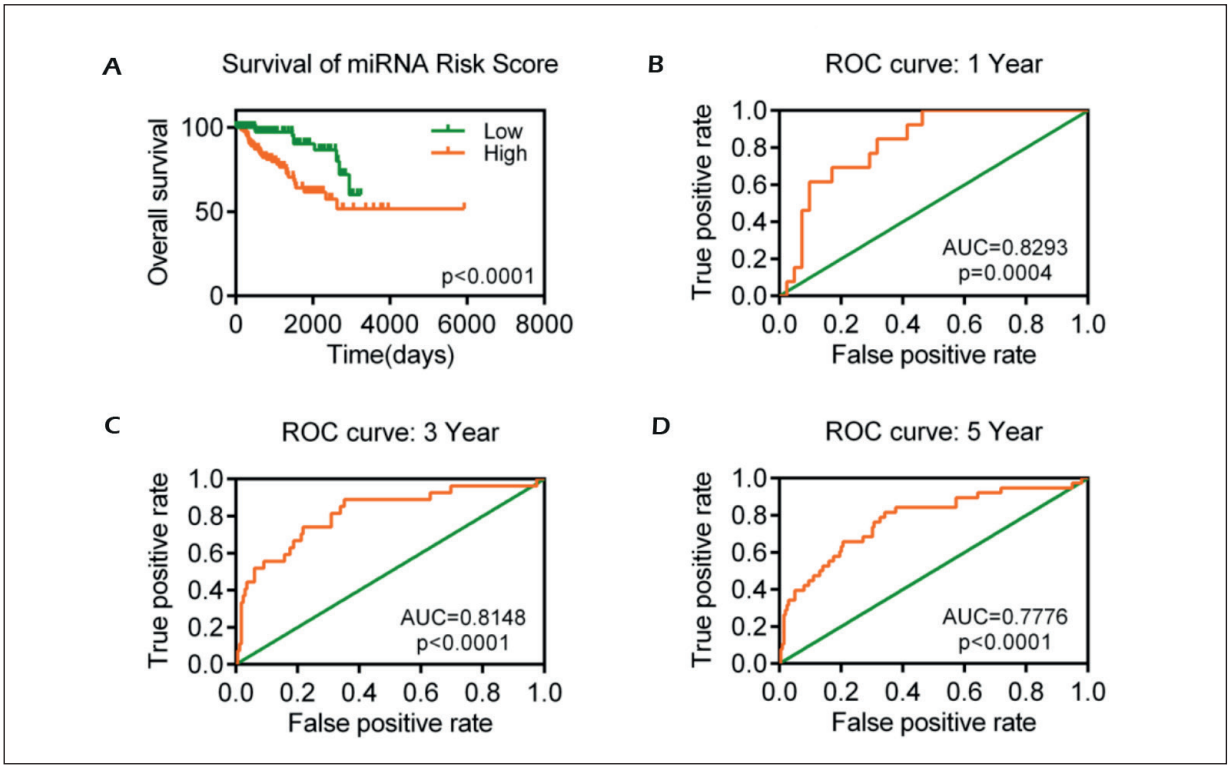

Figure 6. Construction of survival risk score system based on miRNAs signature. **A,** The survival curve of patients with high risk and low risk. **B-D,** The ROC curve in 1-year (**B**), 3-year (**C**), and 5-year (**D**) with AUC value.

tivariate Cox regression analysis, we constructed miRNA prognostic model dependent on hsa-miR-24-1-5p, hsa-miR-34a-5p, and hsa-miR-181c-5p; mRNA prognostic model dependent on SATB2 and ZNF385B. The patients with low risk score of those 3 DEMs and 2 DEGs prognostic model exhibited good survival rate and higher AUC values which suggested that both miRNAs and mRNAs prognostic model could be a good predictor for KIRP. Chang et al[29] indicated that hsa-miR-34a-5p is down-regulated in human cancers. Chen et al (2018)[30] found that hsa-miR-34a-5p is one of top three downregulated miRNAs, and also found that hsa-miR-34a-5p could inhibit brainstem gliomas cell invasion. Haghi et al (2019)[31] also found that miR-34a and miR-16 could collaborate in breast tumor suppression. In the present study, we also found hsa-miR-34a-5p was significantly decreased in KIRP. For the studies on hsa-miR-34a-5p, Gallelli et al (2019)[32] found that hsa-miR-34a-5p and hsa-miR-375 could be recognized as biomarkers for monitoring the effects of drug treatment for migraine pain in children and adolescents. In addition, previous studies also indicated that hsa-miR-181c-5p is upregulated in cemento-ossifying fibroma[33]. This expression trend of hsa-miR-181c-5p was the same as what we found in KIRP.

Consistent with previous researches, our results indicated that 3 DEMs and 2 DEGs were correlated with the OS in KIRP. The time-dependent ROC curve for those 3 DEMs and 2 DEGs had area under curve value higher than 0.5, which suggests that the prognostic model may be good predictors for KIRP. Further analysis including methylation and mutations in related genes could be considered as another dimensional factor to improve the accuracy of our prediction results.

Conclusions

In summary, we identified several prognostic biomarkers for KIRP based on miRNAs-mRNAs network and Cox regression analysis, and constructed 2 models by using 3 miRNAs and 2 mRNAs to predict the prognosis for KIRP patients. Our research reinforced understanding for pathogenesis of KIRP and laid the foundation for future clinical research.

Conflict of Interest
The Authors declare that they have no conflict of interests.

Acknowledgements
This project is financially supported by the Natural Science Foundation of Hunan Province (2019JJ40204), Education Department Foundation of Hunan Province (19A354), Huaihua Science and Technology Department (2020R3104), China Postdoctoral Science Foundation (2020TQ0365), and Hunan Provincial Science & Technology Department (2020SK51202).

Authors' Contribution
Y.L., and X.X., conceived and designed the experiments; Z.Y., and C.X. performed the analysis; Y.Y., C.X., and T.Z. helped to analyze the data; Y.L., and X.X., wrote the paper..

Competing Financial Interests
The authors declare no competing financial interests.

Data Availability Statement
The data that support the findings of this study are openly available in TCGA at https://portal.gdc.cancer.gov/.

References

1) Siegel RL, Miller KD, Jemal A. Cancer statistics, 2019. CA Cancer J Clin 2019; 69: 7-34.
2) Linehan WM, Ricketts CJ. The Cancer Genome Atlas of renal cell carcinoma: findings and clinical implications. Nat Rev Urol 2019; 16: 539-552.
3) Gupta K, Miller JD, Li JZ, Russell MW, Charbonneau C. Epidemiologic and socioeconomic burden of metastatic renal cell carcinoma (mRCC): a literature review. Cancer Treat Rev 2008; 34: 193-205.
4) Porta C, Cosmai L, Leibovich BC, Powles T, Gallieni M, Bex A. The adjuvant treatment of kidney cancer: a multidisciplinary outlook. Nat Rev Nephrol 2019; 15: 423-433.
5) Labrousse-Arias D, Martinez-Alonso E, Corral-Escariz M, Bienes-Martinez R, Berridy J, Serrano-Oviedo L, Conde E, Garcia-Bermejo ML, Gimenez-Bachs JM, Salinas-Sanchez AS, Sanchez-Prieto R, Yao M, Lasa M, Calzada MJ. VHL promotes immune response against renal cell carcinoma via NF-kappaB-dependent regulation of VCAM-1. J Cell Biol 2017; 216: 835-847.
6) Hsieh JJ, Purdue MP, Signoretti S, Swanton C, Albiges L, Schmidinger M, Heng DY, Larkin J, Ficarra V. Renal cell carcinoma. Nat Rev Dis Primers 2017; 3: 17009.
7) Park I, Cho YM, Lee JL, Ahn JH, Lee DH. Prognostic tissue biomarker exploration for patients with metastatic renal cell carcinoma receiving vascular endothelial growth factor receptor tyrosine kinase inhibitors. Tumour Biol 2016; 37: 4919-4927.
8) Nukui A, Masuda A, Abe H, Arai K, Yoshida KI, Kamai T. Increased serum level of soluble interleukin-2 receptor is associated with a worse response of metastatic clear cell renal cell carcinoma to interferon alpha and sequential VEGF-targeting therapy. BMC Cancer 2017; 17: 372.
9) van Kuijk SJA, Parvathaneni NK, Niemans R, van Gisbergen MW, Carta F, Vullo D, Pastorekova S, Yaromina A, Supuran CT, Dubois LJ, Winum JY, Lambin P. New approach of delivering cytotoxic drugs towards CAIX expressing cells: a concept of dual-target drugs. Eur J Med Chem 2017; 127: 691-702.
10) Szendroi A, Szasz AM, Kardos M, Tokes AM, Idan R, Szucs M, Kulka J, Nyirady P, Szendroi M, Szallasi Z, Gyorffy B, Timar J. Opposite prognostic roles of HIF1alpha and HIF2alpha expressions in bone metastatic clear cell renal cell cancer. Oncotarget 2016; 7: 42086-42098.
11) Winter J, Jung S, Keller S, Gregory RI, Diederichs S. Many roads to maturity: microRNA biogenesis pathways and their regulation. Nat Cell Biol 2009; 11: 228-234.
12) Khan AQ, Ahmed EI, Elareer NR, Junejo K, Steinhoff M, Uddin S. Role of miRNA-regulated cancer stem cells in the pathogenesis of human malignancies. Cells 2019; 8: 840.
13) Ardekani AM, Naeini MM. The role of MicroRNAs in human diseases. Avicenna J Med Biotechnol 2010; 2: 161-179.
14) Chen J, Zhang D, Zhang W, Tang Y, Yan W, Guo L, Shen B. Clear cell renal cell carcinoma associated microRNA expression signatures identified by an integrated bioinformatics analysis. J Transl Med 2013; 11: 169.
15) Heinzelmann J, Henning B, Sanjmyatav J, Posorski N, Steiner T, Wunderlich H, Gajda MR, Junker K. Specific miRNA signatures are associated with metastasis and poor prognosis in clear cell renal cell carcinoma. World J Urol 2011; 29: 367-373.
16) Huang da W, Sherman BT, Lempicki RA. Systematic and integrative analysis of large gene lists using DAVID bioinformatics resources. Nat Protoc 2009; 4: 44-57.
17) Fan CN, Ma L, Liu N. Systematic analysis of lncRNA-miRNA-mRNA competing endogenous RNA network identifies four-lncRNA signature as a prognostic biomarker for breast cancer. J Transl Med 2018; 16: 264.
18) Yao Y, Zhang T, Qi L, Liu R, Liu G, Wang J, Song Q, Sun C. Comprehensive analysis of prognostic biomarkers in lung adenocarcinoma based on aberrant lncRNA-miRNA-mRNA networks and Cox regression models. Biosci Rep 2020; 40.
19) Patard JJ, Kim HL, Lam JS, Dorey FJ, Pantuck AJ, Zisman A, Ficarra V, Han KR, Cindolo L, De La Taille A, Tostain J, Artibani W, Dinney CP, Wood CG, Swanson DA, Abbou CC, Lobel B,

Mulders PF, Chopin DK, Figlin RA, Belldegrun AS. Use of the University of California Los Angeles integrated staging system to predict survival in renal cell carcinoma: an international multicenter study. J Clin Oncol 2004; 22: 3316-3322.

20) Zhu H, Lu J, Zhao H, Chen Z, Cui Q, Lin Z, Wang X, Wang J, Dong H, Wang S, Tan J. Functional long noncoding RNAs (lncRNAs) in clear cell kidney carcinoma revealed by reconstruction and comprehensive analysis of the lncRNA-miRNA-mRNA regulatory network. Med Sci Monit 2018; 24: 8250-8263.

21) Ma C, Olevian D, Miller C, Herbst C, Jayachandran P, Kozak MM, Chang DT, Pai RK. SATB2 and CDX2 are prognostic biomarkers in DNA mismatch repair protein deficient colon cancer. Mod Pathol 2019; 32: 1217-1231.

22) Yu W, Ma Y, Shankar S, Srivastava RK. Role of SATB2 in human pancreatic cancer: Implications in transformation and a promising biomarker. Oncotarget 2016; 7: 57783-57797.

23) Conner JR, Hornick JL. SATB2 is a novel marker of osteoblastic differentiation in bone and soft tissue tumours. Histopathology 2013; 63: 36-49.

24) Elgaaen BV, Olstad OK, Sandvik L, Odegaard E, Sauer T, Staff AC, Gautvik KM. ZNF385B and VEGFA are strongly differentially expressed in serous ovarian carcinomas and correlate with survival. PLoS One 2012; 7: e46317.

25) Lee RC, Feinbaum RL, Ambros V. The C. elegans heterochronic gene lin-4 encodes small RNAs with antisense complementarity to lin-14. Cell 1993; 75: 843-854.

26) Mitchell PS, Parkin RK, Kroh EM, Fritz BR, Wyman SK, Pogosova-Agadjanyan EL, Peterson A, Noteboom J, O'Briant KC, Allen A, Lin DW, Urban N, Drescher CW, Knudsen BS, Stirewalt DL, Gentleman R, Vessella RL, Nelson PS, Martin DB, Tewari M. Circulating microRNAs as stable blood-based markers for cancer detection. Proc Natl Acad Sci U S A 2008; 105: 10513-10518.

27) Sohn W, Kim J, Kang SH, Yang SR, Cho JY, Cho HC, Shim SG, Paik YH. Serum exosomal microRNAs as novel biomarkers for hepatocellular carcinoma. Exp Mol Med 2015; 47: e184.

28) Amin MB, Greene FL, Edge SB, Compton CC, Gershenwald JE, Brookland RK, Meyer L, Gress DM, Byrd DR, Winchester DP. The Eighth Edition AJCC Cancer Staging Manual: Continuing to build a bridge from a population-based to a more "personalized" approach to cancer staging. CA Cancer J Clin 2017; 67: 93-99.

29) Chang TC, Wentzel EA, Kent OA, Ramachandran K, Mullendore M, Lee KH, Feldmann G, Yamakuchi M, Ferlito M, Lowenstein CJ, Arking DE, Beer MA, Maitra A, Mendell JT. Transactivation of miR-34a by p53 broadly influences gene expression and promotes apoptosis. Mol Cell 2007; 26: 745-752.

30) Chen X, Dong D, Pan C, Xu C, Sun Y, Geng Y, Kong L, Xiao X, Zhao Z, Zhou W, Huang L, Song Y, Zhang L. Identification of Grade-associated MicroRNAs in brainstem gliomas based on microarray data. J Cancer 2018; 9: 4463-4476.

31) Haghi M, Taha MF, Javeri A. Suppressive effect of exogenous miR-16 and miR-34a on tumorigenesis of breast cancer cells. J Cell Biochem 2019; 120: 13342-13353.

32) Gallelli L, Cione E, Peltrone F, Siviglia S, Verano A, Chirchiglia D, Zampogna S, Guidetti V, Sammartino L, Montana A, Caroleo MC, De Sarro G, Di Mizio G. Hsa-miR-34a-5p and hsa-miR-375 as biomarkers for monitoring the effects of drug treatment for migraine pain in children and adolescents: a pilot study. J Clin Med 2019; 8.

33) Pereira T, Brito JAR, Guimaraes ALS, Gomes CC, de Lacerda JCT, de Castro WH, Coimbra RS, Diniz MG, Gomez RS. MicroRNA profiling reveals dysregulated microRNAs and their target gene regulatory networks in cemento-ossifying fibroma. J Oral Pathol Med 2018; 47: 78-85.